



Quantitative Brain MRI Signal Differences in Children with Congenital Portosystemic Shunt Based on 3D T1-Weighted Sequence

Ying Zhou ¹, Chen Guo¹, Ming Zhu¹, Su-Zhen Dong ^{1,*}

¹ Department of Radiology, Shanghai Children's Medical Center, School of Medicine, Shanghai Jiao Tong University, Shanghai, China

* Corresponding author: Department of Radiology, Shanghai Children's Medical Center, School of Medicine, Shanghai Jiao Tong University, Shanghai, China. Email: dongsuzhen@126.com

Received 2023 December 31; Revised 2024 May 7; Accepted 2024 May 11.

Abstract

Background: Different degrees of T1-weighted (T1W) signal intensities in certain locations on brain magnetic resonance imaging (MRI) are characteristic features of neurological involvement in congenital portosystemic shunt (CPSS). Long-term accumulation of manganese (Mn) as a biomarker can lead to irreversible brain damage.

Objectives: The aim of this study was to utilize quantitative brain MRI indicators to characterize brain signal differences in various regions in children with congenital portosystemic shunt. This may contribute to diagnosis, prognosis, and treatment decisions.

Patients and Methods: This was a case-control study. Thirty-two patients diagnosed with CPSS based on at least one of the following imaging studies—abdominal ultrasound, Digital Subtraction Angiography (DSA), and Computed Tomography (CT)—and who underwent brain MRI prior to interventional treatment or surgery were included as the Case Group in this study. The age of these patients varied from 22 months to 15 years. Brain MRI of thirty children aged 2 to 15 years, identified without liver or structural diseases, were selected as the Control Group. The brain imaging protocol included an axial spin-echo T1-weighted image (T1WI), an axial T2-weighted image (T2WI), an axial diffusion-weighted imaging (DWI), an axial T2-fluid attenuated inversion recovery (FLAIR) sequence, and a sagittal gradient-echo 3D T1W thin-slice sequence, which can be reconstructed into axial and coronal planes. We utilized quantitative MRI assessment based on the 3D T1-weighted sequence to evaluate intracranial signal differences. The quantitative index was categorized into two types: Globus pallidus-to-frontal subcortical white matter Index (GFI) and anterior pituitary-to-pons Index (API). GFI and API were measured and statistically analyzed on the 3D T1W sequence between the Case Group and the Control Group. GFI of the Case Group was also measured and analyzed between the 3D T1W sequence and the standard T1W sequence. Correlation analysis was applied between the GFI ratios and ammonia levels, as well as between the API ratios and ammonia levels in the Case Group. The duration of the study was more than three months.

Results: Significant differences in GFI and API were observed in the Case Group compared with the Control Group ($P < 0.01$). There was also a statistical difference in GFI between the 3D T1W sequence and the standard T1W sequence ($P < 0.01$). However, the GFI and API ratios were not correlated with ammonia levels ($P > 0.05$). The Pearson correlation values were 0.147 and 0.190, respectively.

Conclusion: There was a correlation between different brain signals and congenital portosystemic shunt. Quantitative MRI assessment based on the 3D T1-weighted sequence could be used to evaluate these brain signal differences. A longitudinal study with multiple measurements would be beneficial for more accurately assessing such differences, enabling timely interventions, reducing complications, and avoiding lifelong drug therapy.

Keywords: Hyperammonemia, Congenital Portosystemic Shunt, MRI, Quantitative Assessment, Central Nervous System, Children

1. Background

Congenital portosystemic shunt (CPSS) is a rare vascular anomaly characterized by various anatomical

connections between the portal venous system and the systemic venous system, first described by Abernethy in 1793 (1, 2). Congenital portosystemic shunt is classified into intrahepatic shunts (IHPS) and extrahepatic shunts

(EHPS) based on the abnormal connection sites (3, 4). Over the past 30 years, with advancements in imaging modalities, CPSS has been increasingly recognized, though it remains underreported (5). Congenital portosystemic shunt may present with one or more concurrent symptoms and complications in childhood and adolescence, including hepatopulmonary syndrome, pulmonary hypertension, liver tumors, and neurological abnormalities, rather than portal hypertension seen in adults (6). In contrast to other complications, the early stages of neurological abnormalities may exhibit subtle manifestations that could potentially be overlooked. There are few series on neurological involvement, with only a few case reports or reviews available (7-9).

Symmetrical variations in T1-weighted signal intensity, primarily confined to the globus pallidus on brain MRI, may suggest neurological involvement. Abnormal T1W hyperintensity on magnetic resonance imaging (MRI) is a biomarker of manganese (Mn) overload. Long-term accumulation can lead to irreversible brain damage (10). Herein, we retrospectively reviewed and used quantitative MRI assessment based on the 3D T1W sequence to evaluate 32 patients with portosystemic shunt-related brain signal differences. The aim of this study was to use quantitative indicators to describe the portosystemic shunt-related brain signal differences in different brain regions on brain MRI, which may contribute to diagnosis, prognosis, and treatment decisions.

2. Objectives

The study aimed to utilize quantitative brain MRI indicators to characterize brain signal differences in various regions in children with congenital portosystemic shunt. This characterization may contribute to diagnosis, prognosis, and treatment decisions.

3. Patients and Methods

3.1. Ethical Review

This study was approved by the Institutional Review Board at our hospital and was performed in accordance with the ethical standards laid down in the 1964 Declaration of Helsinki and its later amendments or comparable ethical standards (Ethical Approval Number: SCMCIRB-K2024001-1).

3.2. Data Collection

We conducted a detailed inquiry using our institution's electronic case record system for all terms associated with CPSS, including pulmonary hypertension, hepatopulmonary syndrome, pulmonary arteriovenous fistula, patent ductus venosus, inferior vena cava interruption, hypoxemia, liver dysfunction, heterotaxy, polysplenia, and symmetrical abnormal signal of the globus pallidus. After reviewing the electronic medical records and corresponding available imaging data, patients were considered for inclusion if they had at least one imaging study identifying the presence of CPSS and had undergone brain MRI before interventional treatment or surgery. The imaging studies included abdominal ultrasound, digital subtraction angiography (DSA), and computed tomography (CT). Patients were excluded if pre-therapy brain MRI was unavailable. Additionally, we excluded cases of intrahepatic CPSS in children under 2 years old, as some small intrahepatic shunts may regress before the age of 3 years.

Congenital portosystemic shunt classifications were based on the new classification from the position papers of the Francophone Network for Vascular Liver Diseases and the French Association for the Study of the Liver (AFEF) and ERN-rare liver in 2022 (Table 1) (11, 12). This classification included two types (IHPS and EHPS) and five subtypes. IHPS included two subtypes: Unique shunt and patent ductus venosus (PDV). Extrahepatic shunts included three subtypes: Side-to-side portal-caval shunt (SS shunt), end-to-side portal-caval shunt (ES shunt) with or without ectopic portal vein, and upstream of the portal vein (CPSS originating from any root of the portal vein and entering the lower part of the inferior vena cava [IVC] below the renal veins or any afferent systemic vein corresponding to mesocaval, mesoiliac, or splenorenal shunt).

Table 1. Classification of Congenital Portosystemic Shunts (The Francophone Network for Vascular Liver Diseases and AFEF, and ERN-rare liver in 2022)

Variables	Values
Intrahepatic CPSS (two types)	
Type I	Unique
Type II	Patent ductus venosus
Extrahepatic CPSS (three types)	
Type I	Side-to-side
Type II	End-to-side with or without ectopic portal vein
Type III	Upstream of the portal vein

Abbreviations: CPSS, congenital portosystemic shunts; AFEF, french association for the study of the liver; ERN, european reference network.

3.3. Study Design

In this case-control study, 32 patients diagnosed with CPSS, including 12 females and 20 males, were enrolled as the Case Group (median age: 6 years and 5 months, age range: 22 months to 15 years). Brain MRIs were performed before any intervention between January 2017 and August 2023.

Considering that age can affect T1W signals in the brain, especially in young children, brain MRIs of thirty age- and gender-matched children (aged 2 to 15 years) were selected as the Control Group. All individuals in the Control Group were identified as having no liver or structural brain diseases through examinations such as brain MRI, developmental assessments, liver function tests, or abdominal and cardiac ultrasounds. The reasons for brain MRI scans in the Control Group included long-term follow-up for prematurity, congenital heart disease, trauma, dizziness, and headaches. Informed consent was routinely obtained before brain MRI, DSA, and CT, and we always observed the privacy rights of human subjects.

3.4. Imaging Protocol

Brain MRI was performed using the Discovery MR750 3.0T scanner (GE Medical Systems, USA) with a thirty-two-channel brain coil. Patients were positioned supine, head-first in the magnet. The average duration of the brain MRI was approximately 20 to 30 minutes. Sedatives were only used for children under three years old or uncooperative ones. The brain imaging sequences included an axial spin-echo T1-weighted sequence (T1W, repetition time/echo time, 450 ms/20 ms), an axial T2-weighted sequence (T2W, 3,225 ms/100 ms), an axial diffusion-weighted imaging (DWI, b value: 1,000 s/mm²), an axial T2-fluid attenuated inversion recovery sequence (T2-FLAIR, 9000 ms/140 ms) with a section thickness of 4 mm and a gap of 1 - 2 mm or no gap, and a sagittal gradient-echo three-dimensional T1W thin slices sequence (3D T1W, 6.4 ms/2.4 ms) with a 1 mm slice thickness and no gap, which can be reconstructed into axial and coronal planes.

Abdominal CT enhancement was performed using the Aquilion ONE dynamic volume CT scanner (TOSHIBA, Japan) with 5 - 10 mm slice thickness and 5 - 10 mm spacing, using maximal intensity projection (MIP) after computer thin-slice reconstruction. The contrast media used was Ultravist (Iopromide Injection), 300 mg I/mL, at a dose of 2 mL/kg body weight.

3.5. Imaging Analysis

In this study, we utilized the quantitative index of MRI to analyze brain signal intensity differences. The

quantitative index was categorized into two types: Globus pallidus-to-frontal subcortical white matter Index (GFI) and anterior pituitary-to-pons Index (API). Brain MRI images taken prior to interventional treatment or surgery were retrieved from the hospital's GE picture archiving and communication systems (PACS) and analyzed using the digital imaging and communications in medicine (DICOM) software viewer.

The GFI and API were measured using the following protocol. The targeted bilateral globus pallidus, bilateral frontal subcortical white matter, anterior pituitary, and pons were identified. Using the provided region of interest (ROI) measurement tool with average areas of 0.20 cm² and 0.20 cm², the signal values were measured as the sum of the right and left globus pallidus and the sum of the right and left frontal subcortical white matter on axial 3D T1W and axial standard T1W sequences, respectively. The average values of the globus pallidus and frontal subcortical white matter were then calculated to determine the GFI. Similarly, the ROI measurement tool with average areas of 0.02 - 0.09 cm² and 0.40 cm² was used for measurements of the anterior pituitary and pons on the sagittal 3D T1W sequence to calculate the API. All signal value measurements were performed by one radiologist, with approximately 30% of the patients independently evaluated by another radiologist and coauthor for quality control. The radiologists performing the quantitative MRI measurements were blinded to the group assignments (Case Group vs. Control Group).

3.6. Statistical Analysis

A single Kolmogorov-Smirnov Test (K-S test) was implemented to test the hypothesis of the normal distribution of samples. It was assumed that there was no significant difference in the index values between two independent samples and between two paired samples. An independent-sample *t*-test was applied for the comparison of GFI and API on the 3D T1W sequence between the Case Group and the Control Group. A paired-sample *t*-test was applied to compare the GFI of the Case Group on the 3D T1W sequence with that on the standard T1W sequence. A P-value < 0.01 was considered statistically significant, while a P-value > 0.01 was considered not statistically significant.

Additionally, Pearson correlation analysis was conducted between the GFI ratios and ammonia levels, as well as the API ratios and ammonia levels in the Case Group. The P-value and Pearson correlation coefficient were obtained and analyzed. The P-value represented

whether the two variables were significantly correlated, with a P-value < 0.05 indicating a significant correlation. The correlation coefficient determined the degree of correlation, categorized as follows: Extremely strong correlation (0.8 - 1.0), strong correlation (0.6 - 0.8), moderate correlation (0.4 - 0.6), weak correlation (0.2 - 0.4), and no correlation (0.0 - 0.2).

Statistical analyses were carried out using SPSS version 26 (IBM Corp. Released 2019. IBM SPSS Statistics for Windows, Version 26.0. Armonk, NY: IBM Corp).

4. Results

A total of thirty-two patients diagnosed with CPSS were classified as the Case Group. Age at diagnosis ranged from 18 months to 15 years. Twelve patients were ≤ 5 years old, eleven were between 5 and 10 years, and nine were between 11 and 15 years. There was a male predominance in these 32 cases (male/female: 20/12 = 1.67) and those with IHPS (male/female: 11/2 = 5.50). However, there was no significant gender predominance in the cases with EHPS. There were also no significant gender distribution differences between IHPS and EHPS according to statistical tests [Fisher's exact probability tests] (P-value 0.062). Of the 13 cases with IHPS, PDV type was the most common (10/13, 77%) (Figure 1A). Of the 19 cases with EHPS, the upstream of the portal vein type was the most common (13/19, 68%) (Figure 2A).

A total of thirty children aged 2 to 15 years were selected as the Control Group. Ten were ≤ 5 years old, ten were between 5 and 10 years, and ten were between 11 and 15 years. There were eighteen boys and twelve girls (male/female ratio = 1.5). The purposes of MRI scanning in the Control Group included long-term follow-up for prematurity in 7 (23%), congenital heart disease in 5 (17%), trauma in 6 (20%), and dizziness and headache in 12 (40%).

In our study, hyperammonemia was found in all cases, but only one patient presented occasional unconsciousness and lethargy; the others were asymptomatic. Four cases were found incidentally without any symptoms, two cases presented with abdominal pain, and one case was found by antenatal ultrasound. Associated complications included 14 cases of hepatopulmonary syndrome, 10 cases of pulmonary hypertension, 7 cases of pulmonary arteriovenous fistula (PAVF), and 4 cases of liver lesions or dysfunction. Other complications included one case each of portal hypertension, cardiac insufficiency, heterotaxy, aproctia with navicular fossa fistula, polycystic kidney, and renal duplication malformation.

Demographic, clinical, and imaging characteristics of the congenital portosystemic shunts Group and the Control Group are summarized in Table 2.

Table 2. Demographic, Clinical and Imaging Characteristics of the Congenital Portosystemic shunts Group and the Control Group^a

Variables	Case group (N = 32)	Control group (N = 30)	P-Value
Gender			
Male	20 (62)	18 (60)	-
Female	12 (38)	12 (40)	-
Age (y)			
≤ 5	12 (38)	10 (33)	-
5-10	11 (34)	10 (33)	
10-15	9 (28)	10 (33)	
Presentations			
Hyperammonemia	32 (100)	-	-
None	4 (13)	-	
Antenatal ultrasound	1 (3)	-	
Abdominal pain	2 (6)	-	
Others	4 (9)	-	
Complications			
Encephalopathy	1 (3)	-	-
Hepatopulmonary syndrome	14 (44)	-	
Pulmonary hypertension	10 (31)	-	
Pulmonary arteriovenous fistula	7 (22)	-	
Liver lesions/dysfunction	4 (13)	-	
Portal hypertension	1 (3)	-	
High-output heart failure	1 (3)	-	
Others	4 (13)	-	
Shunt classification			
EHPS	19 (59)	-	
Upstream type	13 (68)	-	
ES type	4 (21)	-	
SS type	2 (11)	-	
IHPS	13 (41)	-	
PDV type	10 (77)	-	
Unique type	3 (23)	-	
Quantitative analysis			
GFI	1.278 ± 0.132	0.969 ± 0.036	< 0.01
API	1.316 ± 0.233	0.941 ± 0.103	< 0.01

Abbreviations: EHPS, extrahepatic shunts; IHPS, intrahepatic shunts; ES, end-to-side; SS: Side-to-Side; PDV, patent ductus venosus; GFI, globus pallidus to white matter of frontal lobe index; API, anterior pituitary to pons index.

^a Values are expressed as No. (%) or. mean ± SD.

The mean GFI of cases in the 3D T1-weighted sequence was 1.278 ± 0.132 (range = 1.001 - 1.494) (Figures 1 and 2B), while this figure was 0.969 ± 0.036 (range = 0.906 - 1.049) in controls (Figure 3A) (P < 0.01). The mean API of cases in the 3D T1-weighted sequence was 1.316 ± 0.233

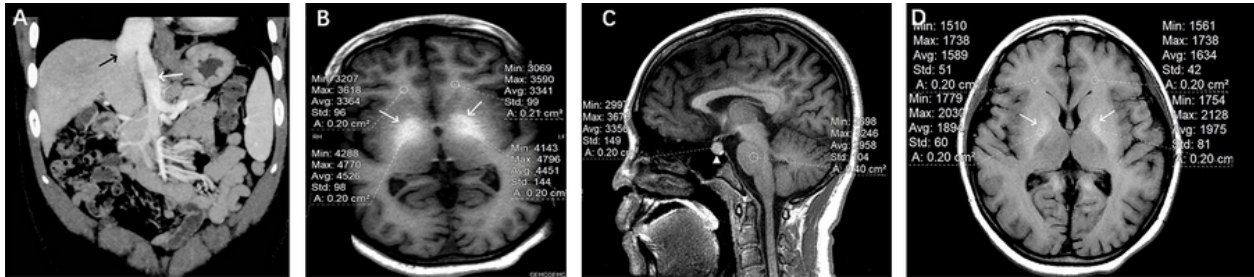


Figure 1. Portosystemic shunt-related brain signal changes in a 11 years old girl with a patent ductus venosus (PDV) shunt (IHPS). A, Abdominal CT angiography showed that after the confluence of the superior mesenteric vein and the splenic vein, it directly entered the inferior vena cava through PDV (white arrow). The inferior vena cava was dilated (black arrow); B, Significantly different signal intensities in the bilateral globus pallidus were noted on axial 3D T1W sequence (white arrows). The globus pallidus-to-white matter of frontal lobe Index (GFI) was 1.339; C, Different signal intensities in the anterior pituitary were described on sagittal 3D T1W sequence (white triangle). The anterior pituitary-to-pons Index (API) was 1.135; D, Different signals in the bilateral globus pallidus were described on axial standard T1W sequence (white arrows). The globus pallidus-to-white matter of frontal lobe Index (GFI) was 1.200.

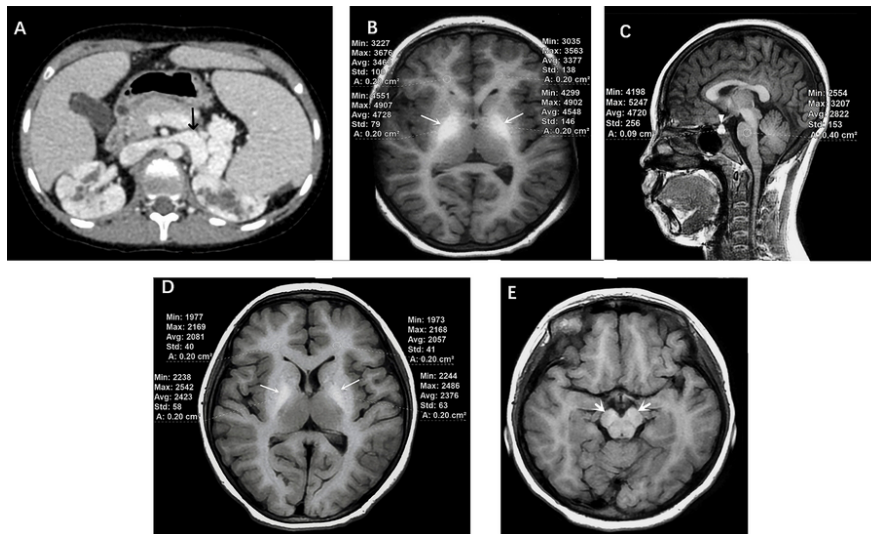


Figure 2. Portosystemic shunt-related brain signal changes in a 13 years old girl with an Upstream of the portal vein type (EHPS). A, Abdominal enhanced CT scan showed that the splenic vein was distorted and dilated, directly entering the inferior vena cava through the left renal vein (black arrow). Bilateral polycystic kidneys were also noted; B, Significantly different signals with larger area in the bilateral globus pallidus were noted on axial 3D T1W sequence (white arrows). The globus pallidus-to-white matter of frontal lobe Index (GFI) was 1.339; C, Different signals in the anterior pituitary were noted on sagittal 3D T1W sequence (white triangle). The anterior pituitary-to-pons Index (API) was 1.698; D, Different signals in the bilateral globus pallidus were described on axial standard T1W sequence (white arrows). The globus pallidus-to-white matter of frontal lobe Index (GFI) was 1.158; E, Different signals in the cerebral peduncle were also noted on axial T1W sequence (white arrows).

(range = 0.804-1.761) (Figures 1 and 2C), while this figure was 0.941 ± 0.103 (range = 0.745 - 1.152) in controls (Figure 3B) ($P < 0.01$). These findings suggest a correlation between different brain signals and portosystemic shunt. In the case group, the mean GFI on the 3D T1W sequence was 1.278 ± 0.132 (range = 1.001 - 1.494), while it was 1.111 ± 0.085 (range = 0.967 - 1.265) on the standard T1W sequence ($P < 0.01$) (Figures 1 and 2D).

Results of GFI and API are presented as Box-Whisker plots in Figures 4A - C.

The P-value and Pearson correlation coefficient between the GFI ratios and ammonia levels in the Case Group were 0.422 and 0.147, respectively. The P-value and Pearson correlation coefficient between the API ratios and ammonia levels in the Case Group were 0.298 and 0.190, respectively. Based on the P-values and correlation

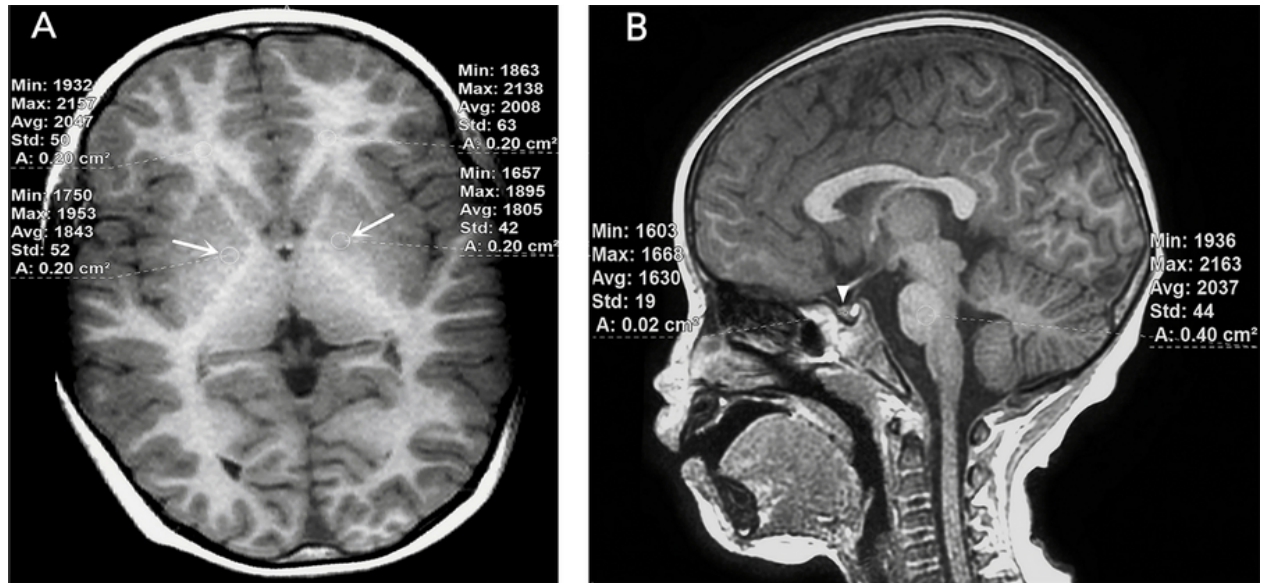


Figure 3. Brain MRI of a 4 years old boy with no liver or structural brain diseases. A, Slight hypointense signals in the bilateral globus pallidus were noted on axial 3D T1W sequence (white arrows). The globus pallidus-to-white matter of frontal lobe Index (GFI) was 0.917; B, Isointense signals were described in the anterior pituitary on sagittal 3D T1W sequence (white triangle).

degrees, it is considered that the GFI and API ratios are not significantly correlated with ammonia levels.

5. Discussion

Over the past decades, CPSS in children has been increasingly recognized due to the rapid development of imaging technologies, but it is still insufficiently understood. The incomplete involution of the embryogenic veins, including the vitelline, cardinal, and umbilical vein systems, affects the development of hepatic sinusoids and leads to abnormal communications between any vein of the portal system and any vein of the inferior vena cava system, based on the anatomical site (right or left, proximal or distal). This allows intestinal blood to bypass the liver, potentially leading to multisystem morbidity. Some small intrahepatic shunts located between the portal branches and hepatic veins may regress and close spontaneously by the age of 1 to 3 years (13-15). However, most shunts, such as persisting intrahepatic shunts, PDV, or extrahepatic shunts, rarely involute and can remain asymptomatic until adulthood (16). In this study, four cases were under 3 years old, including three cases of EHPS and one case of IHPS. Based on the anatomical classifications and the evident clinical manifestations such as hepatopulmonary syndrome (HPS), pulmonary

hypertension (PHTN), and liver dysfunction, intervention therapy was adopted.

In early CPSS cases, some atypical symptoms or complications such as HPS, PHTN, and PAVF were noted instead of liver lesions or portal hypertension, which are typically not liver-related. Moreover, under most conditions, asymptomatic shunts were detected fortuitously on an abdominal ultrasound or abnormal liver function tests performed for other purposes (17), often delaying referral and diagnosis (18).

This case series revealed that hyperammonemia with or without symptoms of portosystemic shunt-related encephalopathy (100%) was the most common presentation. Pulmonary involvement, including HPS (44%), PHTN (31%), and pulmonary arteriovenous fistula (PAVF, 22%), was the main complication.

Neurological abnormalities in CPSS differ from hepatic encephalopathy in adults, which is secondary to portosystemic shunts related to liver cirrhosis or portal vein occlusion. Therefore, "portosystemic encephalopathy" is a more appropriate term to describe the neurological abnormalities and/or hyperammonemia caused by CPSS in childhood or adolescence. Portosystemic encephalopathy is a complex neuropsychiatric syndrome that includes not only asymptomatic/subtle hyperammonemia

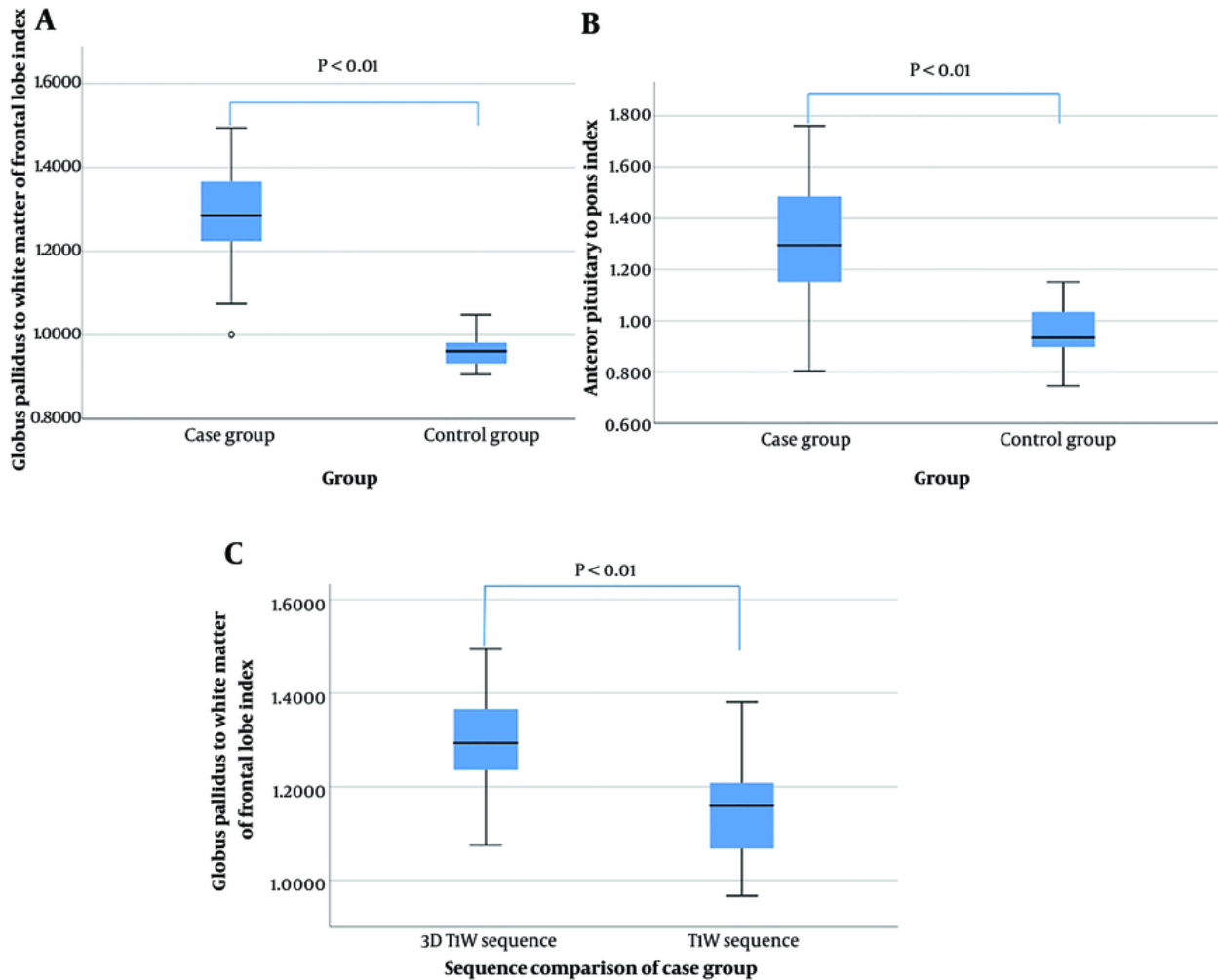


Figure 4. Results of GFI and API were presented as Box-Whisker plots. A, Comparison of GFI between cases and controls; B, Comparison of API between cases and controls; C, Comparison of GFI between 3D T1W sequence and the standard T1W sequence in cases (GFI: Globus pallidus to white matter of frontal lobe index; API: Anterior pituitary to pons index).

encephalopathy but also unexplained cognitive impairment, speech delay, behavioral problems, and learning difficulties, as reported in other studies (19, 20). In the early stages of CPSS, it always exhibits subtle neurological abnormalities but may lead to irreversible brain damage. Studies have revealed that remittent and progressive blood ammonia levels are characteristic of CPSS-related hyperammonemia (16, 21), but they do not reliably correlate with the degree of encephalopathy; rather, the peak and duration of hyperammonemia are more relevant (22, 23). In our study, all 32 cases were accompanied by hyperammonemia, but only one showed portosystemic encephalopathy. In this case,

venous ammonia was moderately elevated, and both the GFI and API were not higher than the mean index values.

Due to the augmented accumulation of manganese, which escapes hepatic clearance in CPSS patients, different degrees of T1-weighted signal intensity can be observed on brain MRI. Commonly involved regions include the globus pallidus, putamen, caudate in the basal ganglia, subthalamic region, dentate nuclei, and cerebral peduncle (Figure 2E). When the disease is extensive, white matter atrophy and anterior pituitary (AP) involvement can also be observed, representing subclinical brain damage (24). Research has shown that long-term involvement can lead to irreversible brain

injury, although the incidence of portosystemic encephalopathy is only about 10%. Abnormal MR signal intensities are (at least partially) reversible in the majority of patients with appropriate management of the shunts and treatment. Therefore, we consider it necessary to have routine brain MRI screening for portosystemic shunt patients, whether or not they exhibit neurological symptoms.

Plasma catecholamines are nervous mediators that include norepinephrine (NE), epinephrine (E), and dopamine (DA). The basal ganglia, particularly the globus pallidus, is the richest area of type 1 and type 2 DA receptors and is the earliest region affected by Mn toxicity, which can lead to extrapyramidal motor dysfunction. Meanwhile, type 2 DA receptors exist on the lactotrophs of the anterior pituitary (AP). As this region lacks a blood-brain barrier, it allows for unrestricted exchange activities, causing instability in the chemical environment. In this study, we selected the globus pallidus and AP to observe the brain involvement of CPSS in children. It showed that both the globus pallidus and AP could be involved in young CPSS patients. Studies in rats with portosystemic hepatic encephalopathy showed that although plasma catecholamines such as E and NE contents were significantly increased, there was no significant change in hypothalamic-AP-dopaminergic activity (25).

The 3D gradient-echo (GE) sequence with high spatial resolution of the brain is often employed in neuroscience and clinical research to obtain structural T1-weighted images. Moreover, quantitative assessment of brain tissues and the volume of individual brain structures have become important tools for more research-oriented applications (26). The typical clinical routine 3D T1W protocols have an isotropic resolution of 1 mm and require a data acquisition time ranging from 4 to 5 minutes. In this study, we measured the signals in the globus pallidus using both the axial 3D T1W sequence and the standard T1W sequence to verify if there was a difference between the ratios. Statistical analysis showed a significant difference in GFI between the 3D T1W sequence and the standard T1W sequence ($P < 0.01$). This difference could be attributed to the thin slice thickness avoiding partial volume issues, excellent tissue contrast, and isotropic resolution, all contributing to a better quantitative assessment.

Because the globus pallidus, frontal lobe, AP, and pons are different sizes, we used an ROI measurement tool with average areas ranging from 0.02 cm² to 0.40 cm² to measure these regions. As the globus pallidus and frontal lobes are bilateral structures, we measured the values on both sides, calculated the average values

of the globus pallidus and frontal lobes, and then calculated the GFI. Additional sequences such as T2-weighted images and diffusion-weighted images may also show signal differences, but to a much lesser extent and are often reported as normal (27, 28).

In this study, we provided a comprehensive description of the characteristics of both the cases and controls, including relevant demographic and clinical information, which helps enhance the understanding of the findings and the P-values between the two groups. However, there were some limitations. This was a retrospective case-control design rather than a prospective study, providing only a snapshot view rather than signal differences over time. This design may potentially impact the results and lead to deviations in the conclusions. To further and accurately assess such differences, a longitudinal study with multiple measurements would be necessary. Additionally, the relatively small patient population ($n = 32$) limited the results of this study. The wide age range also influenced the ratios of the results, although age-matched controls were used. Inadequate brain MRI data after DSA or surgery made it incapable of statistically comparing the singular differences before and after therapy.

Subsequently, more adequately powered controlled studies are required for future investigations, including a more detailed natural history or clinical manifestations delineation, exploring the correlation between the complications and the CPSS classifications, and comparing the intracranial signal differences pre- and post-therapy. Unfortunately, due to the rarity of this disease, a long-term and challenging multidisciplinary team collaborative study is necessary for future medical progress.

In conclusion, the T1W signal intensity of the globus pallidus and anterior pituitary showed varying degrees of difference on brain MRI in children with CPSS compared to controls. Quantitative MRI assessment based on the 3D T1-weighted sequence could be used to evaluate portosystemic shunt-related brain signal differences. A longitudinal study with multiple measurements would be necessary to more accurately assess these differences, take timely interventions, reduce complications, and avoid long-term drug therapy.

Acknowledgements

The authors wish to thank Prof. Qi-Min Chen for his inspiration. Prof. Biao Gong, Prof. Zhao-Hui Deng, Dr. Jing-Qin Zeng, Dr. Xiao-Hong Gu, Hui-Hong Pan, Hong Zhang, Yi Lin for their help with the manuscript.

Footnotes

Authors' Contributions: Study concept and design: M.Z., and S.Z.D.; acquisition of data: Y.Z., and C.G.; analysis and interpretation of data: Y.Z., and C.G.; drafting of the manuscript: Y.Z.; critical revision of the manuscript for important intellectual content: S.Z.D.; statistical analysis: Y.Z.; administrative, technical, and material support: M.Z.; study supervision: S.Z.D.

Conflict of Interests Statement: Authors declared no conflict of interests.

Data Availability: The dataset presented in the study is available on request from the corresponding author during submission or after publication. The data are not publicly available due to privacy restriction.

Ethical Approval: We accepted all regulations of the Helsinki Protocol in our study. The Ethical Approval Number: SCMCIRB-K2024001-1

Funding/Support: This study was supported in part by grant YG2023ZD22 from the Fundamental Research Funds for the Central Universities (Dr Su-Zhen Dong).

Informed Consent: Informed consent was routinely obtained before brain MRI, DSA, and CT, and we always observed the privacy rights of human subjects.

References

- Abernethy J. Account of Two Instances of Uncommon Formation in the Viscera of the Human Body: From the Philosophical Transactions of the Royal Society of London. *Med Facts Obs.* 1797;7:100-8. [PubMed ID: 29106224]. [PubMed Central ID: PMC511139].
- Baiges A, Turon F, Simon-Talero M, Tasayco S, Bueno J, Zekrini K, et al. Congenital Extrahepatic Portosystemic Shunts (Abernethy Malformation): An International Observational Study. *Hepatology.* 2020;71(2):658-69. [PubMed ID: 31211875]. <https://doi.org/10.1002/hep.30817>.
- Blanc T, Guerin F, Franchi-Abella S, Jacquemin E, Pariente D, Soubrane O, et al. Congenital portosystemic shunts in children: a new anatomical classification correlated with surgical strategy. *Ann Surg.* 2014;260(1):188-98. [PubMed ID: 24169154]. <https://doi.org/10.1097/SLA.000000000000266>.
- Kanazawa H, Nosaka S, Miyazaki O, Sakamoto S, Fukuda A, Shigeta T, et al. The classification based on intrahepatic portal system for congenital portosystemic shunts. *J Pediatr Surg.* 2015;50(4):688-95. [PubMed ID: 25840084]. <https://doi.org/10.1016/j.jpedsurg.2015.01.009>.
- DiPaola F, Trout AT, Walther AE, Gupta A, Sheridan R, Campbell KM, et al. Congenital Portosystemic Shunts in Children: Associations, Complications, and Outcomes. *Dig Dis Sci.* 2020;65(4):1239-51. [PubMed ID: 31549332]. [PubMed Central ID: PMC8180198]. <https://doi.org/10.1007/s10620-019-05834-w>.
- Wakamoto H, Manabe K, Kobayashi H, Hayashi M. Subclinical portal-systemic encephalopathy in a child with congenital absence of the portal vein. *Brain Dev.* 1999;21(6):425-8. [PubMed ID: 10487479]. [https://doi.org/10.1016/S0387-7604\(99\)00049-2](https://doi.org/10.1016/S0387-7604(99)00049-2).
- Ortiz M, Cordoba J, Alonso J, Rovira A, Quiroga S, Jacas C, et al. Oral glutamine challenge and magnetic resonance spectroscopy in three patients with congenital portosystemic shunts. *J Hepatol.* 2004;40(3):552-7. [PubMed ID: 15123374]. <https://doi.org/10.1016/j.jhep.2004.01.013>.
- Bartlett JA, Kohli R. Hepatic Encephalopathy in Children. *Indian J Pediatr.* 2024;91(3):280-5. [PubMed ID: 37310582]. [PubMed Central ID: PMC10867031]. <https://doi.org/10.1007/s12098-023-04679-6>.
- Watanabe A. Portal-systemic encephalopathy in non-cirrhotic patients: classification of clinical types, diagnosis and treatment. *J Gastroenterol Hepatol.* 2000;15(9):969-79. [PubMed ID: 11059925]. <https://doi.org/10.1046/j.1440-1746.2000.02283.x>.
- Uchino A, Noguchi T, Nomiya K, Takase Y, Nakazono T, Nojiri J, et al. Manganese accumulation in the brain: MR imaging. *Neuroradiology.* 2007;49(9):715-20. [PubMed ID: 17624522]. <https://doi.org/10.1007/s00234-007-0243-z>.
- Guerin F, Franchi-Abella S, McLin V, Ackermann O, Girard M, Cervoni JP, et al. Congenital portosystemic shunts: Vascular liver diseases: Position papers from the francophone network for vascular liver diseases, the French Association for the Study of the Liver (AFEF), and ERN-rare liver. *Clin Res Hepatol Gastroenterol.* 2020;44(4):452-9. [PubMed ID: 32279979]. <https://doi.org/10.1016/j.clinre.2020.03.004>.
- Bahadori A, Kuhlmann B, Debray D, Franchi-Abella S, Wacker J, Beghetti M, et al. Presentation of Congenital Portosystemic Shunts in Children. *Children (Basel).* 2022;9(2). [PubMed ID: 35204963]. [PubMed Central ID: PMC8870378]. <https://doi.org/10.3390/children9020243>.
- Papamichail M, Pizani M, Heaton N. Congenital portosystemic venous shunt. *Eur J Pediatr.* 2018;177(3):285-94. [PubMed ID: 29243189]. [PubMed Central ID: PMC5816775]. <https://doi.org/10.1007/s00431-017-3058-x>.
- Franchi-Abella S, Gonzales E, Ackermann O, Branchereau S, Pariente D, Guerin F, et al. Congenital portosystemic shunts: diagnosis and treatment. *Abdom Radiol (NY).* 2018;43(8):2023-36. [PubMed ID: 29730740]. <https://doi.org/10.1007/s00261-018-1619-8>.
- Bernard O, Franchi-Abella S, Branchereau S, Pariente D, Gauthier F, Jacquemin E. Congenital portosystemic shunts in children: recognition, evaluation, and management. *Semin Liver Dis.* 2012;32(4):273-87. [PubMed ID: 23397528]. <https://doi.org/10.1055/s-0032-1329896>.
- Ferrero GB, Porta F, Biamino E, Mussa A, Garelli E, Chiappe F, et al. Remittent hyperammonemia in congenital portosystemic shunt. *Eur J Pediatr.* 2010;169(3):369-72. [PubMed ID: 19618212]. <https://doi.org/10.1007/s00431-009-1031-z>.
- Chocarro G, Amesty MV, Encinas JL, Vilanova Sanchez A, Hernandez F, Andres AM, et al. Congenital Portosystemic Shunts: Clinic Heterogeneity Requires an Individual Management of the Patient. *Eur J Pediatr Surg.* 2016;26(1):74-80. [PubMed ID: 26528850]. <https://doi.org/10.1055/s-0035-1566097>.
- Witters P, Maleux G, George C, Delcroix M, Hoffman I, Gewillig M, et al. Congenital veno-venous malformations of the liver: widely variable clinical presentations. *J Gastroenterol Hepatol.* 2008;23(8 Pt 2):e390-4. [PubMed ID: 17868331]. <https://doi.org/10.1111/j.1440-1746.2007.05156.x>.
- Kim MJ, Ko JS, Seo JK, Yang HR, Chang JY, Kim GB, et al. Clinical features of congenital portosystemic shunt in children. *Eur J Pediatr.* 2012;171(2):395-400. [PubMed ID: 21912894]. <https://doi.org/10.1007/s00431-011-1564-9>.
- McLin VA, Franchi-Abella S, Debray D, Guerin F, Beghetti M, Savale L, et al. Congenital Portosystemic Shunts: Current Diagnosis and Management. *J Pediatr Gastroenterol Nutr.* 2019;68(5):615-22. [PubMed ID: 30628988]. <https://doi.org/10.1097/MPG.0000000000002263>.

21. Lux D, Naito A, Harikrishnan S. Congenital extrahepatic portosystemic shunt with progressive myelopathy and encephalopathy. *Pract Neurol*. 2019;**19**(4):368-71. [PubMed ID: 31048365]. <https://doi.org/10.1136/practneurol-2018-002111>.
22. Sokollik C, Bandsma RH, Gana JC, van den Heuvel M, Ling SC. Congenital portosystemic shunt: characterization of a multisystem disease. *J Pediatr Gastroenterol Nutr*. 2013;**56**(6):675-81. [PubMed ID: 23412540]. <https://doi.org/10.1097/MPG.0b013e31828b3750>.
23. Takama Y, Nakamura T, Santo K, Yoneda A. Liver resection for a congenital intrahepatic portosystemic shunt in a child with hyperammonemia and hypermanganesemia: a case report. *Surg Case Rep*. 2020;**6**(1):73. [PubMed ID: 32303849]. [PubMed Central ID: PMC7165232]. <https://doi.org/10.1186/s40792-020-00838-5>.
24. Tuschl K, Mills PB, Clayton PT. Manganese and the brain. *Int Rev Neurobiol*. 2013;**110**:277-312. [PubMed ID: 24209443]. <https://doi.org/10.1016/B978-0-12-410502-7.00013-2>.
25. Scorticati C, Perazzo JC, Rettori V, McCann SM, De Laurentiis A. Role of ammonia and nitric oxide in the decrease in plasma prolactin levels in prehepatic portal hypertensive male rats. *Neuroimmunomodulation*. 2006;**13**(3):152-9. [PubMed ID: 17119344]. <https://doi.org/10.1159/000097260>.
26. Falkovskiy P, Brenner D, Feiweier T, Kannengiesser S, Marechal B, Kober T, et al. Comparison of accelerated T1-weighted whole-brain structural-imaging protocols. *Neuroimage*. 2016;**124**(Pt A):157-67. [PubMed ID: 26297848]. <https://doi.org/10.1016/j.neuroimage.2015.08.026>.
27. Hanquinet S, Morice C, Courvoisier DS, Cousin V, Anooshiravani M, Merlini L, et al. Globus pallidus MR signal abnormalities in children with chronic liver disease and/or porto-systemic shunting. *Eur Radiol*. 2017;**27**(10):4064-71. [PubMed ID: 28386718]. <https://doi.org/10.1007/s00330-017-4808-x>.
28. Quadri M, Federico A, Zhao T, Breedveld GJ, Battisti C, Delnooz C, et al. Mutations in SLC30A10 cause parkinsonism and dystonia with hypermanganesemia, polycythemia, and chronic liver disease. *Am J Hum Genet*. 2012;**90**(3):467-77. [PubMed ID: 22341971]. [PubMed Central ID: PMC3309204]. <https://doi.org/10.1016/j.ajhg.2012.01.017>.